

Lawrence Berkeley National Laboratory

Recent Work

Title

RESONANT RAMAN STUDY OF TRIGONAL Se

Permalink

<https://escholarship.org/uc/item/6xd158p8>

Author

Yu, P.Y.

Publication Date

1976

U U J 4 4 0 3 2 0 0

Submitted to Physical Review

LBL-4598
Preprint

RESONANT RAMAN STUDY OF TRIGONAL Se

P. Y. Yu, N. Amer, Y. R. Shen, and Y. Petroff

RECEIVED
LAWRENCE
BERKELEY LABORATORY

January 1976

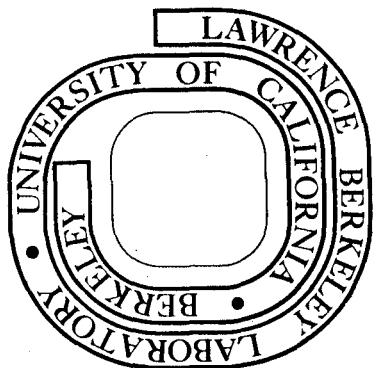
MAR 24 1978

LIBRARY AND
DOCUMENTS SECTION

Prepared for the U. S. Energy Research and
Development Administration under Contract W-7405-ENG-48

For Reference

Not to be taken from this room



LBL-4598
C.1

DISCLAIMER

This document was prepared as an account of work sponsored by the United States Government. While this document is believed to contain correct information, neither the United States Government nor any agency thereof, nor the Regents of the University of California, nor any of their employees, makes any warranty, express or implied, or assumes any legal responsibility for the accuracy, completeness, or usefulness of any information, apparatus, product, or process disclosed, or represents that its use would not infringe privately owned rights. Reference herein to any specific commercial product, process, or service by its trade name, trademark, manufacturer, or otherwise, does not necessarily constitute or imply its endorsement, recommendation, or favoring by the United States Government or any agency thereof, or the Regents of the University of California. The views and opinions of authors expressed herein do not necessarily state or reflect those of the United States Government or any agency thereof or the Regents of the University of California.

To be submitted to The Physical Review

LBL-4598

UNIVERSITY OF CALIFORNIA
Lawrence Berkeley Laboratory
Berkeley, California

AEC Contract No. W-7405-eng-48

RESONANT RAMAN STUDY OF TRIGONAL Se

P. Y. Yu

IBM Thomas J. Watson Research Center
Yorktown Heights, New York 10598

and

N. Amer⁺, Y. R. Shen⁺ and Y. Petroff⁺⁺
Department of Physics, University of California, and
Materials and Molecular Research Division,
Lawrence Berkeley Laboratory, Berkeley, California 94720

JANUARY 1976

⁺Research supported by Energy Research and Development Administration.

^{*}On leave from University of Paris, France.

RESONANT RAMAN STUDY OF TRIGONAL Se

P. Y. Yu

IBM Thomas J. Watson Research Center
Yorktown Heights, New York 10598 andN. Amer⁺, Y. R. Shen⁺ and Y. Petroff^{+,*}Physics Department, University of California, and
Inorganic Materials Research Division, Lawrence Berkeley
Laboratory, Berkeley, California 94720

ABSTRACT: Resonant Raman scattering has been studied in trigonal Se at low temperatures in the region of its indirect and direct excitonic absorption edge. Whereas no enhancement in Raman cross sections was observed at the indirect absorption edge, strong dispersion was found in the region of the direct excitons. In the vicinity of the direct absorption edge Raman cross sections of one phonon modes decreased monotonically with increase in photon energy in all three scattering configurations studied. Only in the scattering configuration where the incident and scattered photons are both polarised perpendicular to the c-axis, resonant enhancements were observed at the direct excitons. This monotonic decrease in Raman cross sections was explained qualitatively by resonant cancellation between a constant background and a dispersive term due to the 2.20 eV peak in the reflectivity spectra of Se. The enhancements in the vicinity of the direct excitons are explained quantitatively by a simple model involving two direct excitons of Se as resonant intermediate states.

We have also determined directly the longitudinal and transverse mode splitting of the low energy E mode in trigonal Se as $7 \pm 2 \text{ cm}^{-1}$.

⁺Research supported by Energy Research and Development Agency.
^{*}On leave from University of Paris, France.

I. INTRODUCTION

Recently resonant Raman scattering (RRS) has been shown to be a powerful new spectroscopic technique which encompasses both traditional optical and Raman spectroscopies and in addition can provide information on electron-phonon interaction in semiconductors.¹ Se, a semiconductor whose properties have been studied extensively² because of its industrial applications, is well suited to resonant Raman studies. This is because trigonal Se has strong anisotropic excitonic absorption peaks lying within the tuning range of available dye lasers. Presently very little is known about the interaction of these excitons with the phonons in Se.

Richter³ has studied RRS in Se at room temperature over a wide range of incident photon frequencies with the discrete lines of various ion lasers augmented by a CW dye laser. Because of the high temperature and discrete tuning nature of that experiment only broad structures in the dispersion of the Raman cross section were observed. In an earlier paper⁴ we have reported low temperature RRS in trigonal Se for incident photon frequencies above its direct absorption edge. In this paper we have extended our measurements below Se's indirect absorption edge. We have also obtained new results which confirm our earlier identification of the $E^{(1)}$ (LO) mode in Se.

II. EXPERIMENTAL DETAILS

Our experiments were performed in a back-scattering configuration using a conventional Raman scattering system which has been described elsewhere.⁵ The Raman spectra were excited by a CW dye laser pumped by an Ar^+ laser. The following dyes from Eastman Kodak: Cresyl Violet

Perchlorate, Rhodamine B and Rhodamine 6G were used to achieve continuous tuning of the dye laser output from 7000 Å to 5500 Å.

The samples we used were single crystalline trigonal Se immersed in superfluid He. As has been reported by Queisser⁶, Se could be damaged by a few milliwatts of laser power in several minutes. This damage process seemed to be quite temperature dependent. From 5°K to 77°K it was observable after one minute or less of irradiation at power densities of less than 10W/cm². At room temperature and at ~ 2°K it required higher laser power density (~ 30 W/cm²) and longer exposure time to observe this effect. This damage results in a decrease in the photoluminescence intensity and a change in the Raman spectrum of Se. By comparing the Raman spectra of the damaged area and that of amorphous Se we conclude that the damage is a result of conversion of Se from the crystalline to the amorphous phase. Furthermore based on the temperature dependence of the damage process we suggest that this process in Se is photo-induced⁷ rather than thermally induced as suggested by Queisser.⁶ Further discussion on this topic is, however, beyond the scope of the present paper. It is important to point out that by keeping the incident laser power low (~ 10mW), by using a cylindrical lens for focussing the laser on the sample and by immersing the sample in superfluid He (T ~ 2°K) we were able to avoid any damage to our samples during the course of our experiments.

Two kinds of Se crystals have been studied. The first kind is a melt-grown bulk single crystal cleaved parallel to the c-axis in liquid nitrogen. The second kind is a thin (~ 100 μ thick) platelet grown from the vapor phase with the c-axis in the plane of the crystal. In both cases the sur-

faces were used without further treatment. In mounting the platelets care was taken to avoid stressing the crystal.

III. OPTICAL, RAMAN AND PHOTOLUMINESCENCE SPECTRA OF Se

Before presenting our RRS results in Se we will review its optical,⁸ Raman⁹ and photoluminescence^{6,10} spectra. These spectra measured on our samples in general agree with those published in the literature so we will not discuss them in detail. However they provide the background information necessary for understanding the RRS results.

(a) Optical Spectra

In Figure 1(a) we show the reflectivity spectra of Se for photon polarisation (\hat{E}_ρ) both parallel and perpendicular to the c-axis. The sharp peak around 1.9 eV is only present in the $\hat{E}_\rho \perp$ c-axis spectrum while the strong peak at 2.20 eV is allowed for both polarisations. Using modulation spectroscopy such as electroreflectance or wavelength modulation techniques⁸ additional structures have been observed at 1.99 eV ($\hat{E}_\rho \perp$ c-axis only) and at 2.003 eV (both polarisations are allowed). Weiser and Stuke⁸ have identified these structures as due to direct excitons associated with transitions occurring at the H point of the Brillouin zone. For future reference we have labelled these direct excitons at 1.948, 1.990, 2.003 and 2.2 eV as a, b, c and d respectively. The absorptivity curves obtained on Se platelets from 1.80 eV up to 1.93 eV are plotted in Figure 1(b). These show steps due to phonon-assisted indirect excitonic absorption as reported by Fischer.⁸ Above 1.93 eV the absorption coefficients were either extrapolated or taken from the data of Tutihasi and Chen.⁸ By comparison with the theoretical band structure¹¹ of Se, Lingelbach et al.¹² have

assigned the indirect exciton to transition from the H point of the valence band to the Z point of the conduction band.

(b) Raman Scattering

The lattice dynamics of trigonal Se have been studied both experimentally,^{9,13} and theoretically¹⁴ by a number of authors. Trigonal Se has space group symmetry D_3^4 and three atoms per unit cell arranged to form chains parallel to the c-axis. The bonding between Se atoms within the same chain is covalent while the interaction between Se atoms in different chains is much weaker. The frequencies and symmetries of the six zone-center optical phonons and their off-resonance Raman selection rules¹⁵ are summarised in Table I. We note that the A_2 and $E^{(1)}$ modes have much lower energies than the nearly degenerate A_1 and $E^{(2)}$ modes. This energy difference is generally explained by the fact that the A_1 and $E^{(2)}$ mode involves mainly the stretching of the covalent bonds while the A_2 and $E^{(1)}$ mode the bending of the bonds.¹⁶

In Figures 2 and 3 we show some typical Raman spectra of our Se samples for photon energies below the indirect absorption edge (off-resonance regime). In Figure 2(a) and (b) we compare the Raman spectra of our two kinds of Se samples obtained in the scattering configuration $\hat{E}_l \parallel \text{c-axis} \perp \hat{E}_s$. Figures 3(a) and (b) show the Raman spectra of the bulk sample for two other scattering configurations: $\hat{E}_l \parallel \hat{E}_s \perp \text{c-axis}$ and $\hat{E}_l \parallel \hat{E}_s \parallel \text{c-axis}$.

In general the off-resonance Raman spectra obtained on our two kinds of Se samples resemble each other and also those reported by Mooradian

and Wright.⁹ The exceptions are the 202 and 211 cm^{-1} peaks. These peaks are present in the bulk sample spectra and were also reported by Mooradian and Wright but they are not observed in the Se platelets. These two peaks are probably extrinsic in nature but without further work they cannot be identified at the present.

In the $\hat{E}_\ell \parallel \text{c-axis} \perp \hat{E}_s$ configuration we found two peaks around 150 cm^{-1} (see Figures 2(a) and 2(b)) with frequencies 147 and 154 cm^{-1} (Raman frequencies given in this paper are accurate to $\pm 2 \text{ cm}^{-1}$ unless otherwise stated). In our earlier paper (reference 4) and in the paper by Mooradian and Wright⁹ only one peak was reported in this region. Mooradian and Wright observed the 147 cm^{-1} peak and identified it as the $E^{(1)}$ transverse optical (TO) mode. In reference 4 a mode was observed at 151 cm^{-1} and based on its resonant scattering it was identified as the $E^{(1)}$ longitudinal optical (LO) mode. We have now been able to observe both modes. We found that for incident photon energy below the direct absorption edge the 147 cm^{-1} mode is easily observable while the 154 cm^{-1} mode is weakly present in the $\hat{E}_\ell \parallel \text{c-axis} \perp \hat{E}_s$ configuration. This probably explains why only the 147 cm^{-1} mode was observed by Mooradian and Wright who excited their Raman spectra with a YAG:Nd laser at 1.06 μ . As the incident photon energy approaches the direct absorption edge the 147 cm^{-1} mode decreases in intensity and becomes undetectable. On the other hand for photon energy above 1.93 eV the 154 cm^{-1} mode becomes strongly enhanced in the configuration $\hat{E}_\ell \parallel \hat{E}_s \perp \text{c-axis}$. As a result we were able to observe only the 154 cm^{-1} mode in reference 4 (the discrepancy of 3 cm^{-1} in the frequency of this mode reported earlier and in this paper is within experimental

uncertainty). These new results support our earlier assignment of the 154 cm^{-1} Raman peak as the $E^{(1)}$ (LO) mode and give directly the TO-LO splitting of the $E^{(1)}$ mode as $7 \pm 2 \text{ cm}^{-1}$ which is in good agreement with the value of 6 cm^{-1} obtained by Lucovsky et al.⁹ from infrared absorption.

The Raman selection rules listed in Table I are in general obeyed in Se when the incident photon energy is below the indirect absorption edge. The exceptions are the appearance of the Raman inactive A_2 mode in the configuration $\hat{E}_\ell \parallel \text{c-axis} \perp \hat{E}_s$ and the occurrence of the 147 cm^{-1} ($E^{(1)}$ (TO)) mode in the $\hat{E}_\ell \parallel \hat{E}_s \parallel \text{c-axis}$ configuration (see Figures 2 and 3(b)). These violations of the selection rules observed in the off-resonance regime are probably due to defects in the crystal.

(c) Photoluminescence

The photoluminescence of Se has been studied by Queisser⁶ and by Zetsche and Fischer.¹⁰ Figure 4 shows the luminescence spectra of our Se samples. The platelet spectrum (Figure 4(a)) is very similar to the 2°K spectrum reported by Zetsche and Fischer.¹⁰ The bulk Se sample spectrum (Figure 4(b)) is lower in intensity and shows mainly one broad shoulder. The differences in the luminescence and Raman spectra between the two kinds of Se samples indicate that the platelets probably have higher quality than the bulk Se crystals.

Fischer⁸ has identified the structures in the photoluminescence spectrum of Se as due to phonon-assisted recombination of the indirect exciton and a hypothetical shallow acceptor. In Figure 4(a) we have indicated by arrows the positions of the phonon-assisted indirect exciton recombination peaks expected from the known zone center optical

and zone edge acoustic phonon energies. Except for the $W_{IE} - E^{(2)}$ peak these peaks explain rather well all the structures in Figure 4(a).

IV. EXPERIMENTAL RESULTS

Due to the strong photoluminescence in the Se platelets, we were not able to measure the RRS in these samples when the incident photon frequencies are in the vicinity of the indirect exciton. As a result the RRS results presented in this paper were obtained on the bulk Se crystals. However, when the Raman signal is not masked by the luminescence, such as when the incident photon is resonant with the direct excitons, we do not find any difference between the two kinds of samples. We believe that the resonant Raman results presented in this paper are intrinsic properties of Se.

We have studied RRS in Se for three scattering configurations:

(a) $\hat{E}_\ell \parallel \hat{E}_s \perp c\text{-axis}$, (b) $\hat{E}_\ell \parallel c\text{-axis} \perp \hat{E}_s$ and (c) $\hat{E}_\ell \parallel \hat{E}_s \parallel c\text{-axis}$.

Our results are shown in Figures 5 and 6.

According to Table I in the configurations $\hat{E}_\ell \parallel \hat{E}_s \perp c\text{-axis}$ only two types of one-phonon Raman modes: E and A_1 are allowed. Since the A_1 and $E^{(2)}$ modes are separated by only 3 cm^{-1} and we have selected a spectral slit width of $\sim 4 \text{ cm}^{-1}$ to obtain the best combination of signal-to-noise ratio and resolution, we were not able to resolve these two modes. As a result we will identify the unresolved 233 cm^{-1} mode in this configuration as the $(A_1, E^{(2)})$ mode.

The Raman cross sections of the 233 cm^{-1} ($A_1, E^{(2)}$); 147 cm^{-1} ($E^{(1)}$ (TO)); 154 cm^{-1} ($E^{(1)}$ (LO)) and 304 cm^{-1} ($2E^{(1)}$ (LO)) modes measured in the configuration $\hat{E}_\ell \parallel \hat{E}_s \perp c\text{-axis}$ are plotted in Figure 5 as a

function of the incident photon energies. The normally Raman inactive 112 cm^{-1} (A_2) mode begins to appear for incident photon energies above 1.94 eV. This mode exhibits resonant enhancement very similar to the $E^{(1)}(\text{LO})$ mode for incident photon energy between 1.94 and 2.03 eV. The RRS results on this A_2 mode have been presented in detail in reference 4 so will not be repeated here.

In the configuration $\hat{E}_\ell \parallel \text{c-axis} \perp \hat{E}_s$ only the E modes are allowed. In this configuration we found that none of the observed Raman modes shows any enhancement. As shown in Figure 6(a) the three E modes: 233 cm^{-1} ($E^{(2)}$); 147 cm^{-1} ($E^{(1)}(\text{TO})$) and 154 cm^{-1} ($E^{(1)}(\text{LO})$) decrease in intensity monotonically with increase in incident photon energy.

$\hat{E}_\ell \parallel \hat{E}_s \parallel \text{c-axis}$ is the only configuration in which we observed enhancement of Raman modes at the d exciton. The modes enhanced are the A_1 and $E^{(1)}(\text{LO})$ modes and their cross-sections are plotted in Figure 6(b) as a function of incident photon energies.

In obtaining the Raman cross sections in Figures 5 and 6 the effect of the absorption coefficient on the scattering intensity has been corrected for in a manner described by Loudon¹⁷. We should point out that in reference 4 this correction was not applied because the absorption coefficients did not vary much in the photon energy range of that paper. But in the present case this absorption correction is important because the absorption coefficients change by several orders of magnitude at the direct absorption edge.

V. DISCUSSIONS

To explain the dispersion in the Raman cross-sections of Se shown in Figures 5 and 6 we have expressed the Raman tensor as a sum of three terms:

$$R(\omega_{\ell}) = A + Bf(\omega_{\ell} - \omega_g) + Cg(\omega_{\ell}) \quad (1)$$

In Eq. (1) the constant A is the off-resonance Raman tensor. It is zero for modes which are forbidden according to Table I (e.g. the A_2 mode). The term $f(\omega_{\ell} - \omega_g)$ is assumed to be a dispersive function arising from a transition at energy $\hbar\omega_g$. Interference between $f(\omega_{\ell} - \omega_g)$ and A will be shown to produce the monotonic decreases in Raman cross sections around the absorption edge. We will therefore consider A and $Bf(\omega_{\ell} - \omega_g)$ together. The function $g(\omega_{\ell})$ contains all the resonant terms due to the direct excitons a, b and c and accounts for the enhancement peaks in the vicinity of these direct excitons.

We will now consider the $A + Bf(\omega_{\ell} - \omega_g)$ and $g(\omega_{\ell})$ terms individually.

$$(1) \quad \underline{A + Bf(\omega_{\ell} - \omega_g)}$$

We can qualitatively explain the monotonic decrease in the Raman cross sections of Se by a resonant cancellation between the constant A and the dispersive term $Bf(\omega_{\ell} - \omega_g)$. As an example we will consider the A_1 mode in the configuration $\hat{E}_{\ell} \parallel \hat{E}_s \parallel$ c-axis. In this configuration the a and b excitons are not optically active so the term $g(\omega_{\ell})$ can be neglected. The Raman cross section of the A_1 mode can be written as:

$$\sigma_{A_1}(\omega_{\ell}) \propto |A + Bf(\omega_{\ell} - \omega_g)|^2 \quad (2)$$

As pointed out by Ralston et al.¹⁸ if the two terms in Eq. (2) tend to

cancel each other as ω_ℓ approaches ω_g the Raman cross section will decrease instead of becoming enhanced. In case $|Bf(\omega_\ell = \omega_g)| > |A| \sigma_{A_1}$ will reach a minimum (anti-resonance) at some photon energy $\hbar\omega_\ell < \hbar\omega_g$ before peaking at $\hbar\omega_g$. This model was used successfully to account anti-resonances observed in the RRS of a number of semiconductors.¹⁸

In Se the A_1 mode seems to show the same kind of behavior. Its cross section first reaches a broad minimum around 1.92 eV and then peaks at 2.20 eV which is the energy of the first strong reflectivity peak in Se for $\hat{E}_\ell \parallel$ c-axis. This suggests that the 2.20 eV reflectivity peak is responsible for the $f(\omega_\ell - \omega_g)$ term and $\hbar\omega_g \sim 2.20$ eV. Noting that this 2.20 eV peak is optically active for both polarisations \parallel and \perp c-axis it is plausible that this peak is also responsible for the monotonic decrease in the other two configurations. The absence of the 2.20 eV peak in the Raman cross sections for the other two configurations can be explained by a smaller $Bf(\omega_\ell - \omega_g)$ term in these cases. If $|Bf(\omega_\ell = \omega_g)| < |A|$ in Eq. (2) the Raman cross section will be minimum at $\hbar\omega_\ell = \hbar\omega_g$ and will not show a peak at $\hbar\omega_g$. This explanation is also consistent with the fact that the 2.20 eV reflectivity peak is stronger for $\hat{E}_\ell \parallel$ c-axis than for $\hat{E}_\ell \perp$ c-axis.

It should be pointed out that for $\hat{E}_\ell \parallel \hat{E}_s \perp$ c-axis the $(A_1, E^{(2)})$ modes show enhancements associated with the a and b excitons so the term $g(\omega_\ell)$ cannot be neglected. However there seems to be no interference between $g(\omega_\ell)$ and the other two terms in Eq. (1) so we can assume that their Raman cross section can be written as:

$$\sigma_{(A_1, E(2))}(\omega_\ell) \propto |A + Bf(\omega_\ell - \omega_g)|^2 + |Cg(\omega_\ell)|^2 \quad (3)$$

The $|A + Bf(\omega_\ell - \omega_g)|^2$ term again accounts for the monotonic decreasing background on which is now superimposed the enhancements due to the direct excitons.

Although the above model explains qualitatively our results, a quantitative comparison between Eq. (2) and experimental results is not possible at present due to our lack of knowledge of the form of $f(\omega_\ell - \omega_g)$. In their model Ralston et al.¹⁸ have used the following expansion for $f(\omega_\ell - \omega_g)$:

$$f(\omega_\ell - \omega_g) = (\omega_\ell - \omega_g)^{1/2} - (\omega_\ell - \omega_g - \omega_{\text{phonon}})^{1/2} \quad (4)$$

which is appropriate if $\hbar\omega_g$ is a three dimensional M_0 -type of energy gap with no exciton effect. We were not able to obtain any reasonable fit to our results with Eq. (4). Since there is no evidence that the 2.20 eV transition in Se is a three dimensional M_0 -type energy gap this is not unexpected. A derivation of $f(\omega_\ell - \omega_g)$ for Se requires a better understanding of the 2.20 eV peak.

Another area where further work is required is understanding the relative signs of A and $Bf(\omega_\ell - \omega_g)$ since these signs determine whether there will be resonant cancellation or not. Although models have been proposed to estimate the relative signs of A and $Bf(\omega_\ell - \omega_g)$, they have very limited success so far.^{18,19}

(2) $g(\omega_\ell)$

In reference 4 we have proposed a simple model involving only the a and b excitons (the c exciton appears to have much smaller oscillator strength so was neglected) as resonant intermediate states to explain the enhancement

of the LO phonons in the vicinity of the a and b excitons. We will now make use of essentially the same model to calculate $g(\omega_\ell)$ for both the $E^{(1)}(\text{LO})$ and the $(A_1, E^{(2)})$ modes.

In Figure 7 we show diagrammatically all the Raman processes involving the a and b excitons as resonant intermediate states. By summing over all four diagrams we obtain an expression for $g(\omega_\ell)$:

$$\begin{aligned}
 g(\omega_\ell) = & \frac{\langle 0 | H_{ER} | a \rangle \langle a | H_{EP} | a \rangle \langle a | H_{ER} | 0 \rangle}{(\omega_\ell - \omega_a - i\Gamma_a)(\omega_s - \omega_a - i\Gamma_a)} + \\
 & \frac{\langle 0 | H_{ER} | b \rangle \langle b | H_{EP} | b \rangle \langle b | H_{ER} | 0 \rangle}{(\omega_\ell - \omega_b - i\Gamma_b)(\omega_s - \omega_b - i\Gamma_b)} + \\
 & \frac{\langle 0 | H_{ER} | b \rangle \langle b | H_{EP} | a \rangle \langle a | H_{ER} | 0 \rangle}{(\omega_\ell - \omega_b - i\Gamma_b)(\omega_s - \omega_a - i\Gamma_a)} + \\
 & \frac{\langle 0 | H_{ER} | a \rangle \langle a | H_{EP} | b \rangle \langle b | H_{ER} | 0 \rangle}{(\omega_\ell - \omega_a - i\Gamma_a)(\omega_s - \omega_b - i\Gamma_b)} \quad (5)
 \end{aligned}$$

where $\hbar\omega_a$, $\hbar\omega_b$, $\hbar\Gamma_a$ and $\hbar\Gamma_b$ are respectively the energies and dampings of the a and b excitons. H_{ER} and H_{EP} represents respectively the exciton-photon and exciton-phonon Hamiltonian. Here it is important to point out the distinction between the longitudinal optical phonon like the $E^{(1)}(\text{LO})$ mode and other optical phonons like the A_1 mode. Whereas all optical phonons interact with excitons via the deformation potential (dp) mechanism, LO phonons have an additional coupling via the Fröhlich interaction.²⁰ For LO phonons with a sizable microscopic field its Fröhlich interaction usually dominates over its dp interaction. Thus we expect for the $E^{(1)}(\text{LO})$ mode H_{EP} would be the Fröhlich Hamiltonian²⁰ while for the $(A_1, E^{(2)})$ mode H_{EP} would be given by the dp Hamiltonian.

The first two terms in Eq. (5) involves either the a or the b

exciton alone so we will refer to them as the intra-exciton terms. The last two terms involve coupling of the a and b excitons via the phonon so they will be called the inter-exciton terms. For the dp Hamiltonian both kinds of terms are in general non-zero. For the Fröhlich Hamiltonian it is well-known that $\langle a | \text{Fröhlich Hamiltonian} | a \rangle$ vanishes²⁰ if the phonon wave vector q is neglected. Thus we expect the inter-exciton terms to be more important for the $E^{(1)}$ (LO) mode.

To compare our experimental results with Eq. (5) we make the usual assumption that the exciton-phonon and exciton-photon matrix elements are constant parameters and write the Raman cross section in the form:

$$\sigma(\omega_\ell) \propto \left| \frac{\alpha}{(\omega_\ell - \omega_a - i\Gamma_a)(\omega_s - \omega_a - i\Gamma_a)} + \frac{\beta}{(\omega_\ell - \omega_b - i\Gamma_b)(\omega_s - \omega_b - i\Gamma_b)} + \frac{\gamma}{(\omega_\ell - \omega_b - i\Gamma_b)(\omega_s - \omega_a - i\Gamma_a)} + \frac{\gamma}{(\omega_\ell - \omega_a - i\Gamma_a)(\omega_s - \omega_b - i\Gamma_b)} \right|^2 \quad (6)$$

In general α , β and γ are complex quantities. For the $(A_1, E^{(2)})$ modes we have assumed that they are all real numbers for the sake of simplicity. For the $E^{(1)}$ (LO) mode α and β are functions of the phonon wave vector q (since the q independent term is zero) and as such they are assumed to be purely imaginary.

The experimental enhancements in the Raman cross sections of the $E^{(1)}$ (LO) and $(A_1, E^{(2)})$ modes have been fitted with Eq. (6) by adjusting the parameters α , β , γ , Γ_a and Γ_b . The exciton energies $\hbar\omega_a = 1.9495$ eV and $\hbar\omega_b = 1.990$ eV are assumed known. The resultant theoretical curves are shown in Figure 8 as the solid lines. Since there are a number of adjustable parameters involved, instead of adjusting them independently, the following procedure was adopted.

By noting that the first peak in the cross section of the $(A_1, E^{(2)})$ mode is determined mainly by the *a* exciton, we let $\gamma = \beta = 0$ initially and fit the experimental results in this region to obtain Γ_a . We found that $\hbar\Gamma_a \simeq 6.2$ meV in good agreement with the width of the *a* exciton peak in the absorption spectrum. Next we try to fit the 1.97 eV peak in the cross section of the $E^{(1)}(\text{LO})$ mode. As pointed out earlier the $E^{(1)}(\text{LO})$ mode enhancement is determined mainly by the inter-exciton terms. We therefore let $\alpha = \beta = 0$ and adjust Γ_b to fit the 1.97 eV peak. We determine $\hbar\Gamma_b \simeq 25$ meV which is consistent with the large width of the *b* exciton in the optical spectra. After Γ_a and Γ_b are determined in these ways only two parameters: α/γ and β/γ are adjusted independently to fit the experimental points.

For the $(A_1, E^{(2)})$ modes we obtain $\alpha/\gamma \simeq 1$ and $\beta/\alpha \simeq -0.015$. For the $E^{(1)}(\text{LO})$ mode the best result we could obtain is shown in Figure 8(b) with $|\alpha|/\gamma \simeq 0.05$ and $|\beta|/\gamma \simeq 0.01$.

These numbers are consistent with our expectation that the inter-exciton terms are responsible for the enhancement of the $E^{(1)}(\text{LO})$ mode. We also note that for both modes the contribution of the *a* exciton to the intra-exciton terms is larger than that of the *b* exciton by a factor of 5 to 6. This is also consistent with the relative strength of these two excitons in absorption.

The agreement between theory and experiment is not too good for the $E^{(1)}(\text{LO})$ mode on the low energy side. This could be explained by the omission of the *a* exciton continuum in our simple model. Martin²⁰ has shown that below the 1s exciton level the contributions to the wave

vector dependent Fröhlich interaction from the exciton continuum will tend to cancel those of the discrete exciton levels. Inclusion of the a exciton continuum in our model will probably improve the agreement between theory and experiment for the $E^{(1)}$ (LO) mode both on the low and high energy side.

VI. RRS AT INDIRECT ENERGY GAPS

Attempts to observe RRS at indirect energy gaps was first made by Scott et al. in GaP.²¹ These authors attributed their failure to observe any enhancement of the one phonon modes at the indirect gap of GaP to the small oscillator strength of the indirect gaps. Recently selective enhancement of two-phonon modes at indirect energy gaps has been reported in Si,²² and AgBr²³ and also in Cu₂O.²⁴ In case of Cu₂O the energy gap is direct but dipole-forbidden so it resembles an indirect gap in that dipole transitions are accompanied by phonon emission or absorption.

In Se we have tried without success to detect selective enhancement of the two-phonon modes at the indirect excitons. A probable reason for the absence of selective RRS in Se and other indirect gap materials²⁵ is due to the proximity of the indirect and direct energy gaps. In these cases the effect of the direct gap tends to overshadow the indirect gap. We note that in materials where such selective RRS has been reported the direct gaps are well separated from the indirect gap. These separations are larger than 2 eV in Si and AgBr and around 0.6 eV in Cu₂O.

VII. CONCLUSION

We have studied RRS in trigonal Se at low temperatures in the vicinity of its indirect and direct excitons. We did not observe any resonance effect associated with the indirect excitons. At the direct absorption

edge the one phonon Raman cross sections were found to decrease with increase in photon energy. Only in the scattering configuration $\hat{E}_i \parallel \hat{E}_s \perp c\text{-axis}$ did we observe resonant enhancements at the direct excitons. The decrease in Raman cross sections was explained qualitatively by resonant cancellation between a constant background and a dispersive contribution from the 2.20 eV peak in the reflectivity spectra of Se. The enhancements due to the direct excitons were explained quantitatively by a simple model involving the 1.95 eV and 1.99 eV excitons of Se as resonant intermediate states.

ACKNOWLEDGEMENT

We would like to thank Mr. J. M. Thuilier (E.N.S., Paris) and Drs. M. Voos and C. Rigeaux for providing us with the Se samples. Technical assistance of J. A. Bradley is also acknowledged. We are also grateful to S. E. Kohn for measuring the reflectivity of Se.

REFERENCES

1. See recent reviews by J. L. Birman in Proceedings of the Twelfth International Conference on the Physics of Semiconductors ed. by M. Pilkuhn, B. G. Teubner, Stuttgart (1974); P. Y. Yu in Proceedings of the Third International Conference on Light Scattering in Solids (to be published) and R. M. Martin and L. M. Falicov, in Light Scattering in Solids ed. by M. Cardona, Springer-Verlag, Heidelberg (1975).
2. See articles in The Physics of Selenium and Tellurium, ed. by W. C. Cooper, Pergamon Press, London (1969).
3. W. Richter in The Proceedings of the Eleventh International Conference on the Physics of Semiconductors, Vol. 2, Polish Scientific Publishers, Warsaw (1972).
4. N. Amer, Y. Petroff, Y. R. Shen and P. Y. Yu, Proceedings of the Twelfth International Conference on the Physics of Semiconductors, ed. by M. Pilkuhn, B. G. Teubner, Stuttgart (1974).
5. P. Y. Yu and Y. R. Shen, Phys. Rev. B12, 1377 (1975).
6. H. J. Queisser in reference 2.
7. Photo-induced crystallization of amorphous Se has been reported by J. Dresner and G. B. Stringfellow, J. Phys. Chem. Solids, 29, 303 (1968) and by J. Feinleib, J. de Neufville, S. C. Moss and S. R. Ovshinsky, Appl. Phys. Letters 18, 254 (1971).
8. R. Fischer, Phys. Rev. B5, 3087 (1972); S. Tutihasi and I. Chen, Phys. Rev. 158, 623 (1967); G. Weiser and J. Stuke, Phys. Stat. Solidi 45b, 691 (1971) and T. O. Tuomi, Phys. Stat. Solidi 38, 623 (1970).

9. A. Mooradian and G. B. Wright, p. 266 of Ref. 2; G. Lucovsky, R. C. Keezer and E. Burstein, Solid State Comm. 5, 439 (1967); G. Lucovsky, A. Mooradian, W. Taylor, G. B. Wright and R. C. Keezer, Solid State Comm. 5 113 (1967).
10. H. Zetsche and R. Fischer, J. Phys. Chem. Solids 30, 1425 (1969).
11. R. Sandrock, Phys. Rev. 169, 642 (1968).
12. W. Lingelbach, J. Stuke, G. Weiser and J. Treusch, Phys. Rev. B5, 243 (1972).
13. W. C. Hamilton, B. Lassier and M. I. Kay, J. Phys. Chem. Solids 35, 1089 (1974).
14. M. Hulin, Ann. Phys. (Paris) 8, 647 (1963); R. Geick and U. Schröder in reference 2; W. D. Teuchert and R. Geick, Phys. Stat. Solidi 61b, 123 (1974).
15. R. Loudon, Adv. Phys. 13, 423 (1964).
16. J. Stuke in reference 2.
17. R. Loudon, J. Phys. Radium 26, 677 (1965).
18. J. M. Ralston, R. L. Wadsack and R. K. Chang, Phys. Rev. Lett. 25, 814 (1970), R. M. Hoff and J. C. Irwin, Phys. Rev. B10, 3464 (1974); R. H. Callender, M. Balkanski and J. L. Birman in Light Scattering in Solids, ed. by M. Balkanski, Flammarion (Paris) 1971; J. L. Lewis, R. L. Wadsack and R. K. Chang ibid; T. C. Damen and J. F. Scott, Solid State Comm. 9, 383 (1971).
19. See M. Cardona, F. Cerderia and T. A. Fjeldly, Phys. Rev. B10, 3433 (1974) and references therein.

20. R. Loudon, Proc. Roy. Soc. A275, 218 (1963); R. M. Martin, Phys. Rev. B4, 3677 (1971).
21. J. F. Scott, T. C. Damen, R. C. C. Leite and W. T. Silvast, Solid State Comm. 7, 953 (1969).
22. P. B. Klein, H. Masui, J. J. Song and R. K. Chang, Solid State Comm. 14, 1163 (1974).
23. W. von der Osten, J. Weber and G. Schaack, Solid State Comm. 15, 1561 (1974).
24. P. Y. Yu, Y. R. Shen, Y. Petroff and L. M. Falicov, Phys. Rev. Lett. 30, 283 (1973); P. Y. Yu and Y. R. Shen, Phys. Rev. B12, 1377 (1975).
25. Although Klein et al. have claimed to observe selective enhancement in the 2T0 phonons of GaP by temperature tuning, we have not been able to observe this effect by using a dye laser to tune across the indirect gap of GaP at room temperature.

TABLE I Symmetry, frequency and Raman selection rules of zone center
Optical phonons of trigonal Se

<u>Mode</u>	<u>Frequency (cm⁻¹)</u>		<u>Raman Selection Rules</u>
	Previous work ⁽¹⁾	Present work	
A ₂ (TO)	112		} Raman inactive
A ₂ (LO)		114	
E ⁽¹⁾ (TO)	147	147	} $\hat{E}_l \parallel \hat{E}_s \perp c\text{-axis}$ and $\hat{E}_l \perp \hat{E}_s$
E ⁽¹⁾ (LO)		154	
E ⁽²⁾	232		
A ₁	235		$\hat{E}_l \parallel \hat{E}_s$

(1) Reference 9.

FIGURE CAPTIONS

1. Optical spectra of trigonal Se at liquid helium temperatures for photon polarization \hat{E}_ℓ both parallel and perpendicular to the c-axis; (a) reflectivity and (b) absorptivity. The parts of the absorptivity curve for $\hat{E}_\ell \perp$ c-axis above 1.93 were obtained from data of Tutihasi and Chen (reference 8). The broken curve is an extrapolation. The indirect exciton energy ω_{IE} and also the energy of the direct exciton a, b and c are indicated by arrows. The latter were obtained from data of Weiser and Stuke (reference 8).
2. Raman spectra of two different kinds of Se crystals: (a) bulk single crystal and (b) platelet. The scattering configurations in both cases are $\hat{E}_\ell \parallel$ c-axis $\perp \hat{E}_s$ and the incident photon energy is 1.818 eV. Numbers above the curves are the relative gain of the amplifier for different parts of the spectra.
3. Raman spectra of bulk Se crystal measured in two different scattering configurations: (a) $\hat{E}_\ell \parallel \hat{E}_s \perp$ c-axis and (b) $\hat{E}_\ell \parallel \hat{E}_s \parallel$ c-axis. The incident photon energy and meaning of the numbers above each curve are the same as in Figure 2.
4. The photoluminescence spectra of (a) Se platelet and (b) bulk Se crystal at $\sim 2^\circ\text{K}$ excited by the dye laser. The intensity for curve (b) is about one order of magnitude lower than for curve (a). The energies of the indirect exciton (ω_{IE}) and its phonon replicas are indicated by arrows. TA and LA are the zone boundary acoustic phonon energies determined by neutron scattering (Ref. 14). The polarization in both curves are perpendicular to the c-axis.

5. Raman cross-section of the $(A_1, E^{(2)})(+)$, $E^{(1)}(TO)(o)$, $E^{(1)}(LO)(\bullet)$ and $2E^{(1)}(LO)(\Delta)$ modes plotted as a function of the incident photon energy. The scattering configuration is $\hat{E}_\ell \parallel \hat{E}_s \perp c\text{-axis}$.
6. Raman cross-section of Se plotted against incident photon energy for two different energy ranges: (a) 1.8-2.0 eV and (b) 2.14-2.25 eV. In (a) the scattering configuration is $\hat{E}_\ell \parallel c\text{-axis} \perp \hat{E}_s$ for the $E^{(2)}(+)$, $E^{(1)}(TO)(o)$ and $E^{(1)}(LO)(\bullet)$ modes and $\hat{E}_\ell \parallel \hat{E}_s \parallel c\text{-axis}$ for the A_1 mode (Δ). In (b) the scattering configuration is $\hat{E}_\ell \parallel \hat{E}_s \parallel c\text{-axis}$ for both the $A_1(\Delta)$ and $E^{(1)}(LO)(\bullet)$ modes.
7. Diagrammatic representations of the four scattering processes which contribute to the RRS in Se at the a and b direct exciton.
8. Comparison between the theoretical curve (solid lines) obtained from Eq. 6 and the experimental points for (a) $(A_1, E^{(2)})$ modes and (b) $E^{(1)}(LO)$ mode. The values of the parameters used in Eq. 6 are given in the text.

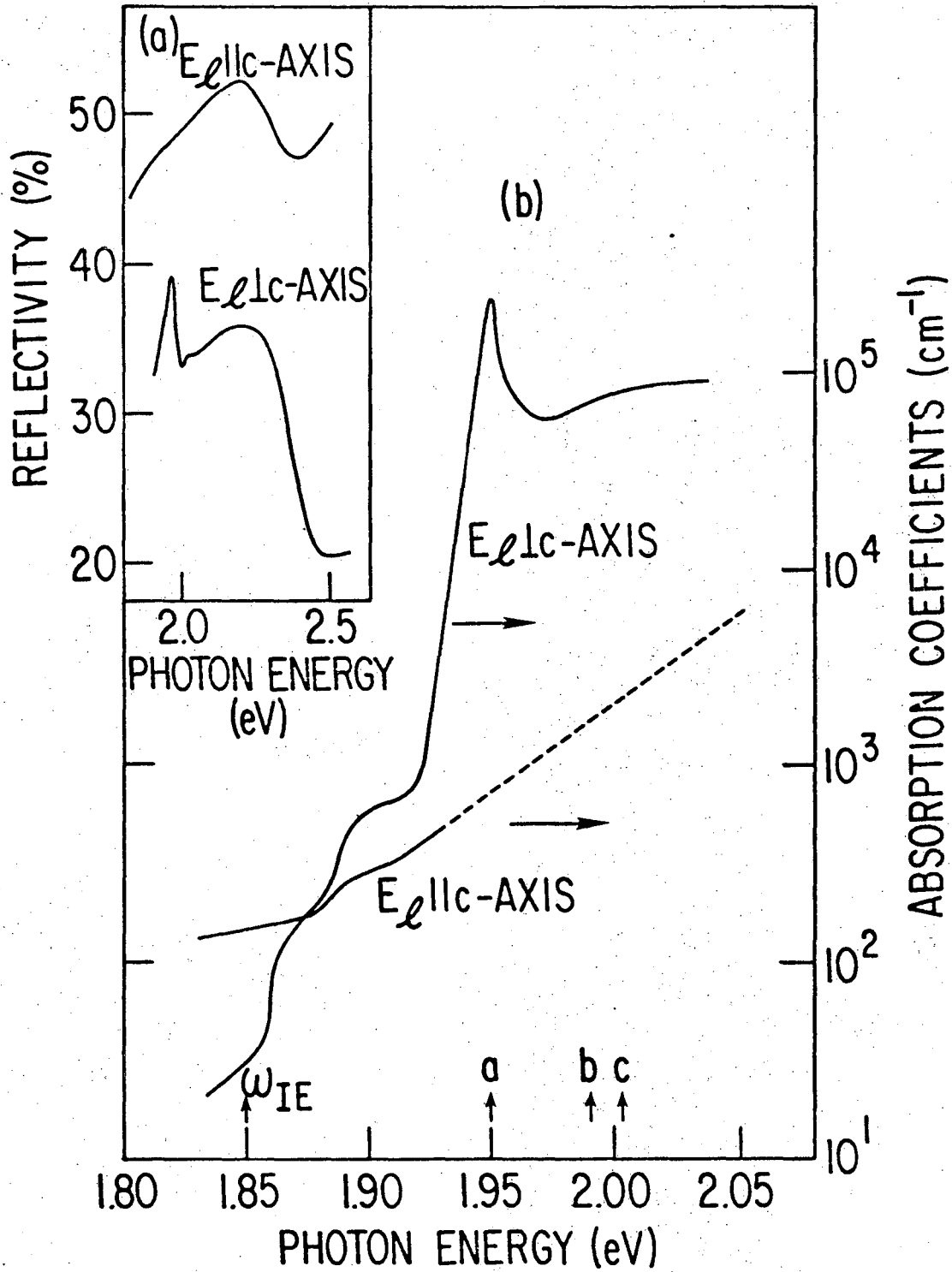


Fig. 1

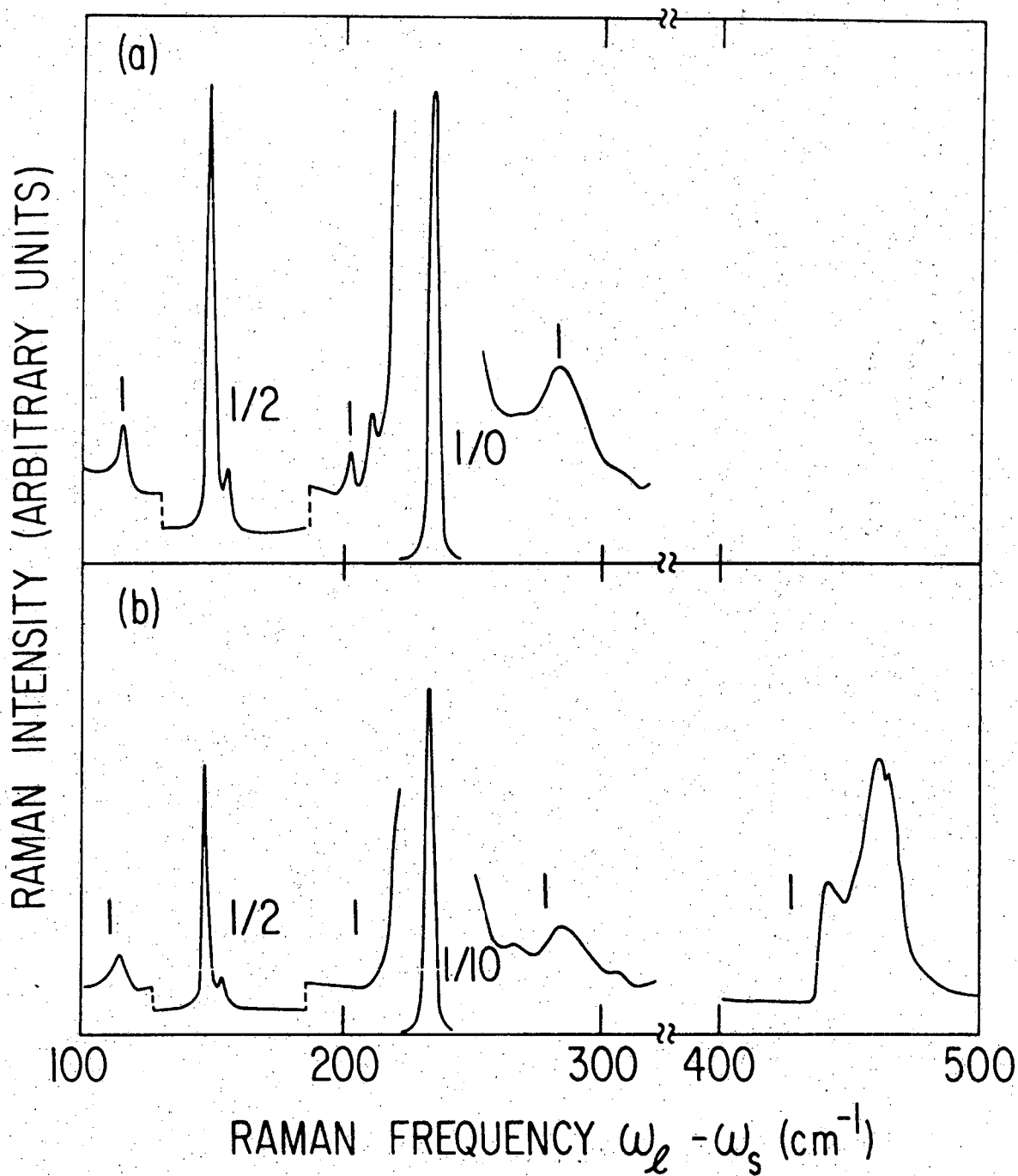


Fig. 2

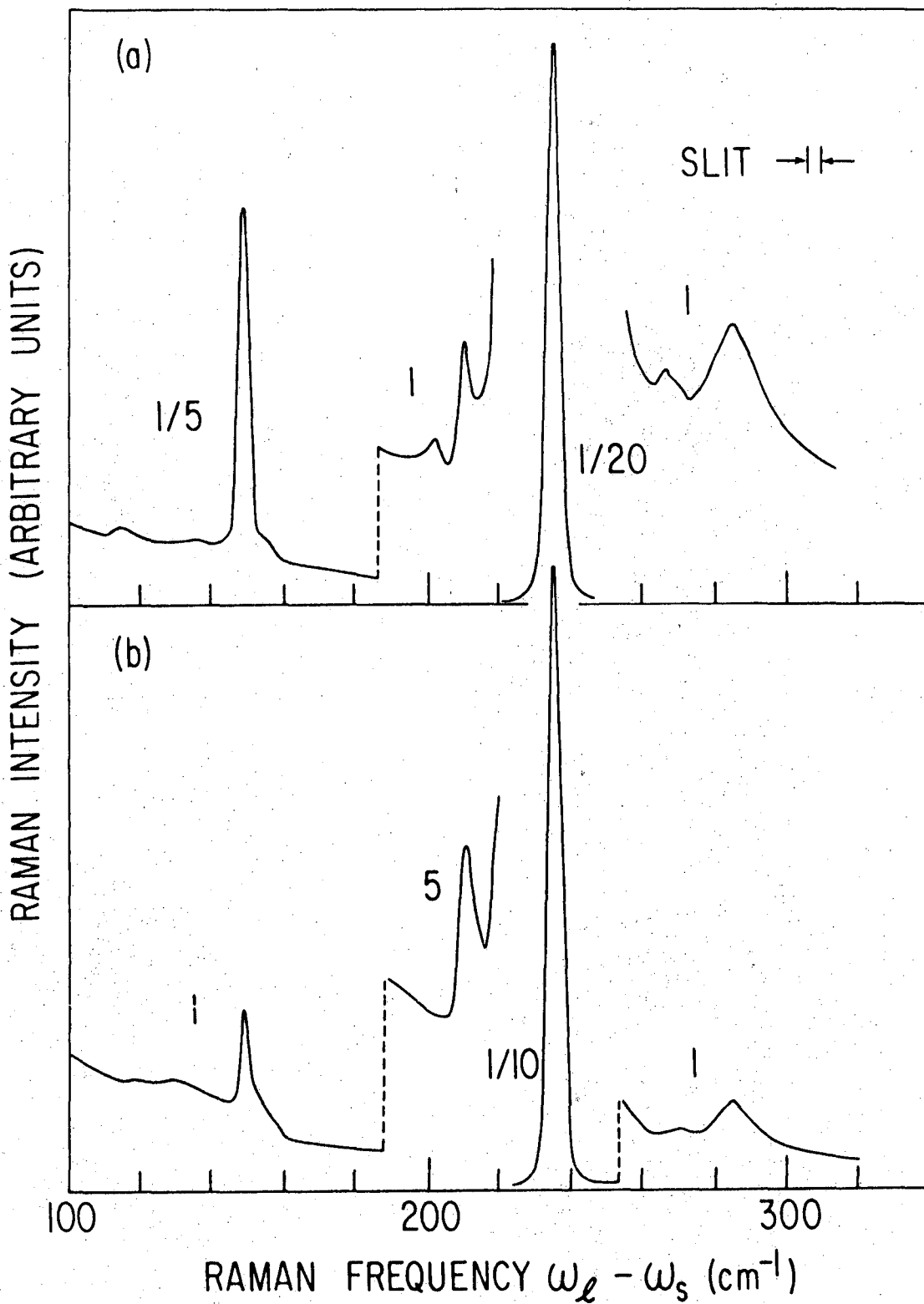


Fig. 3

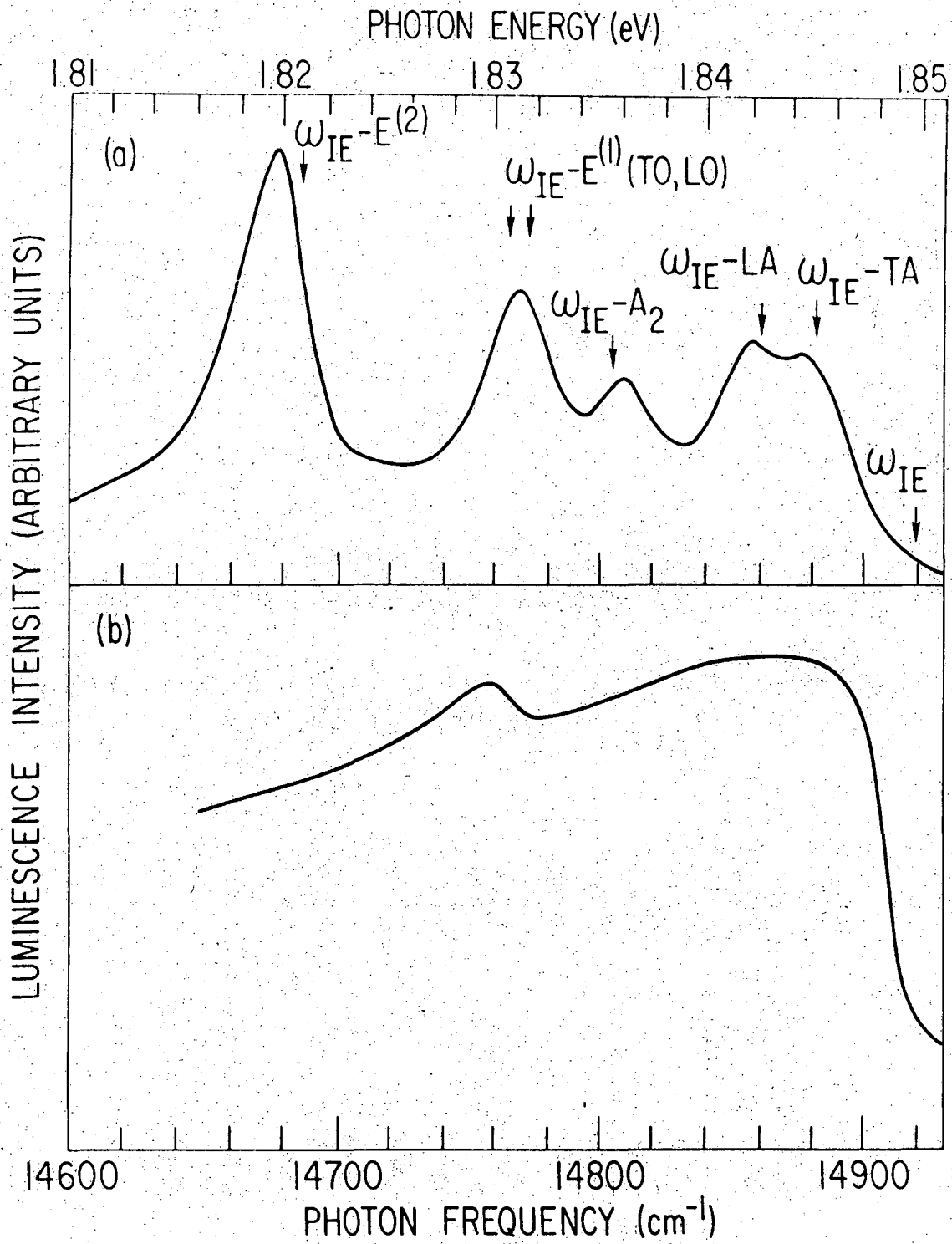


Fig 4

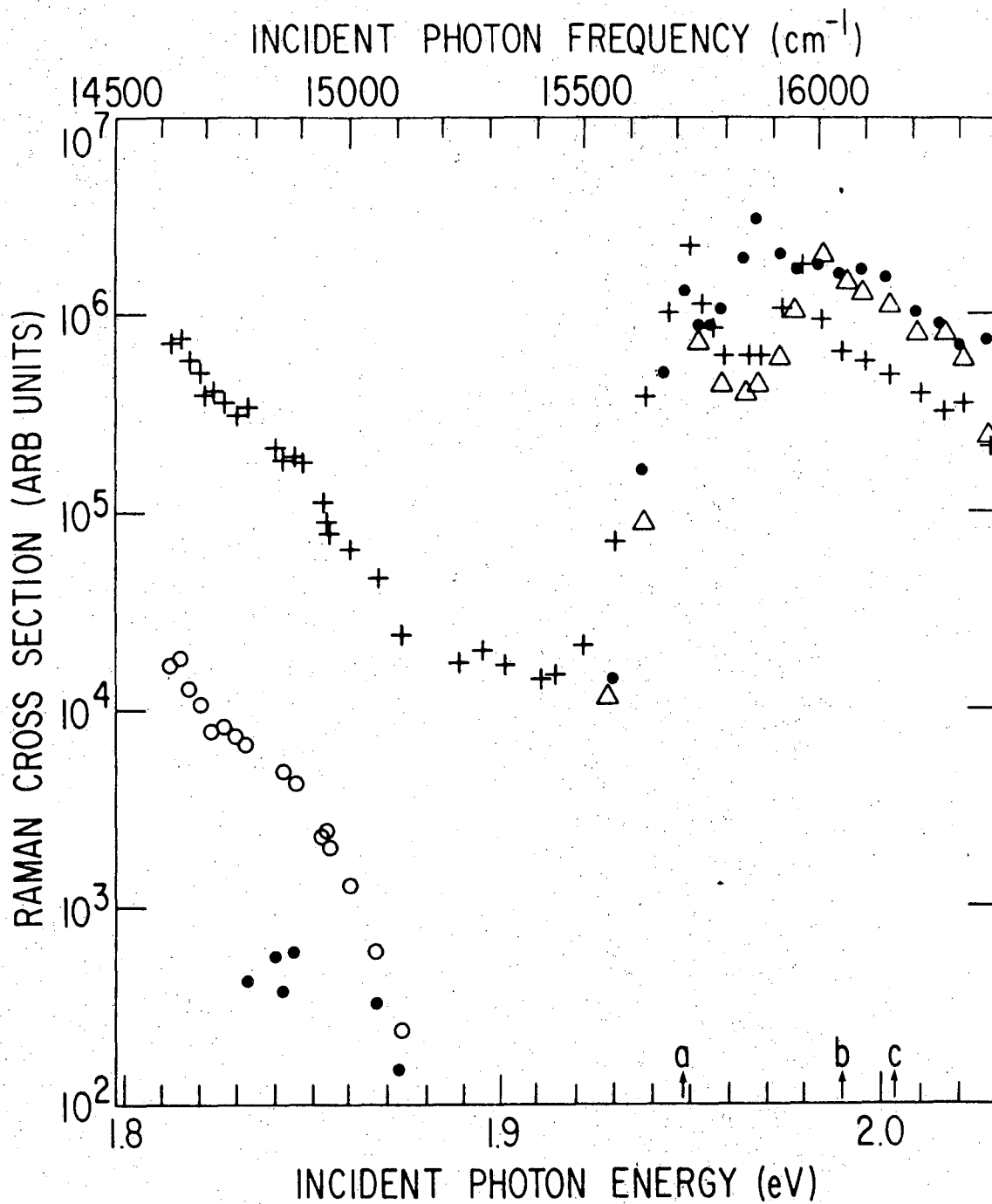


Fig. 5

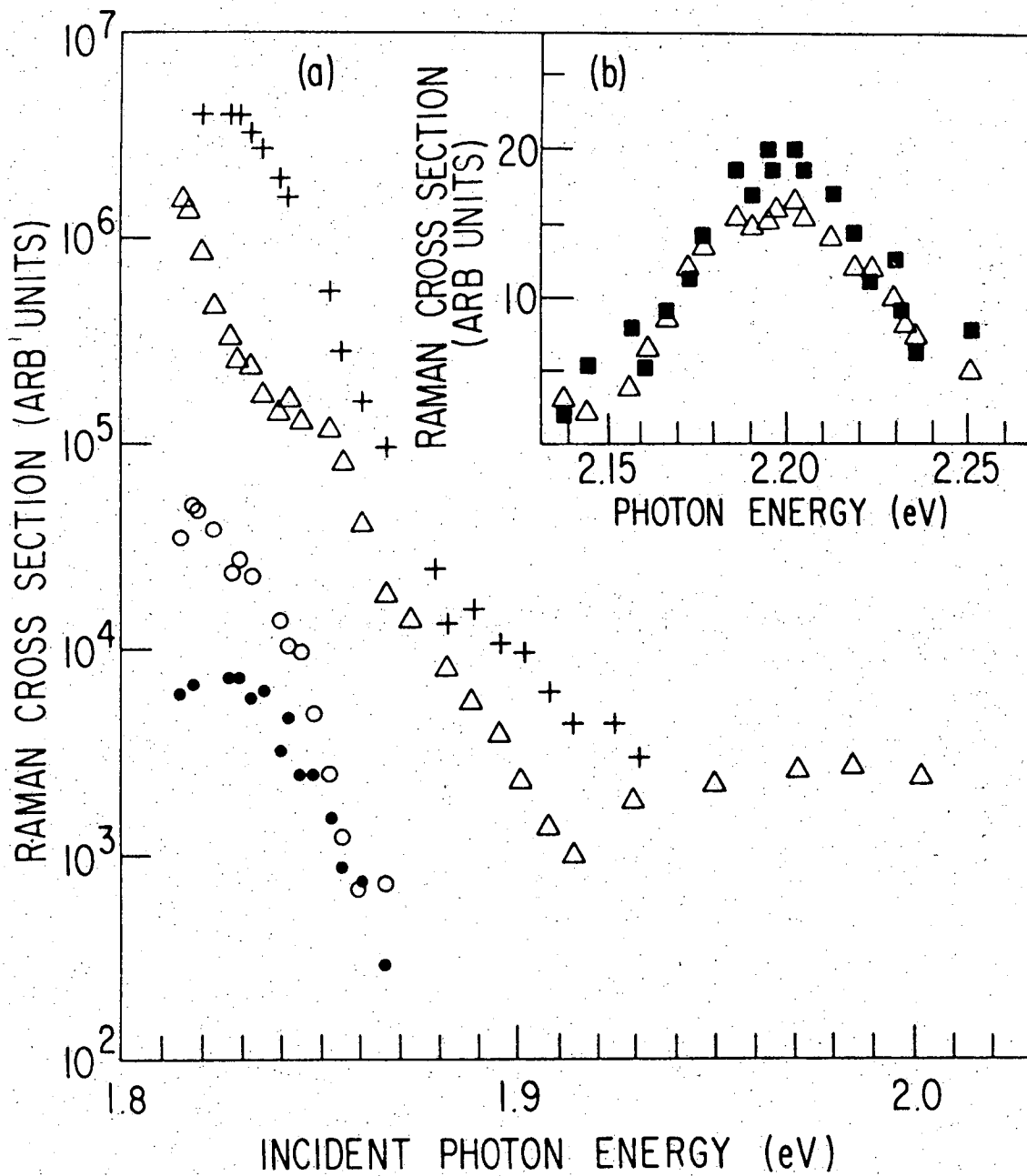






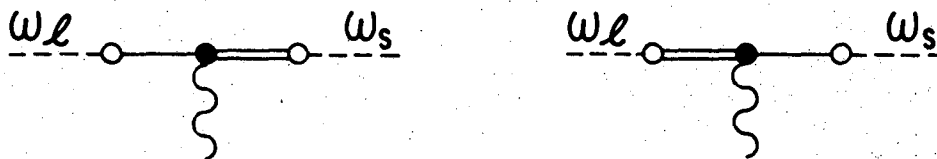


Fig. 6

NOTATIONS:

	a	EXCITON
	b	EXCITON
	H_{ER}	PHOTON-EXCITON INTERACTION
	H_{EP}	PHONON-EXCITON INTERACTION
		PHOTON
		PHONON

INTER-EXCITON SCATTERING



INTRA-EXCITON SCATTERING

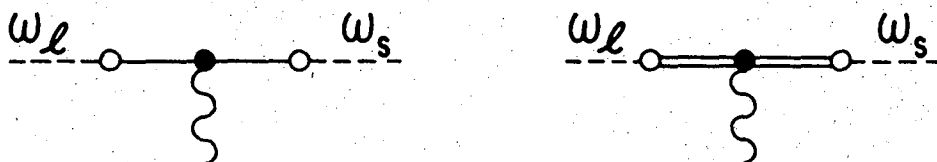


Fig. 7

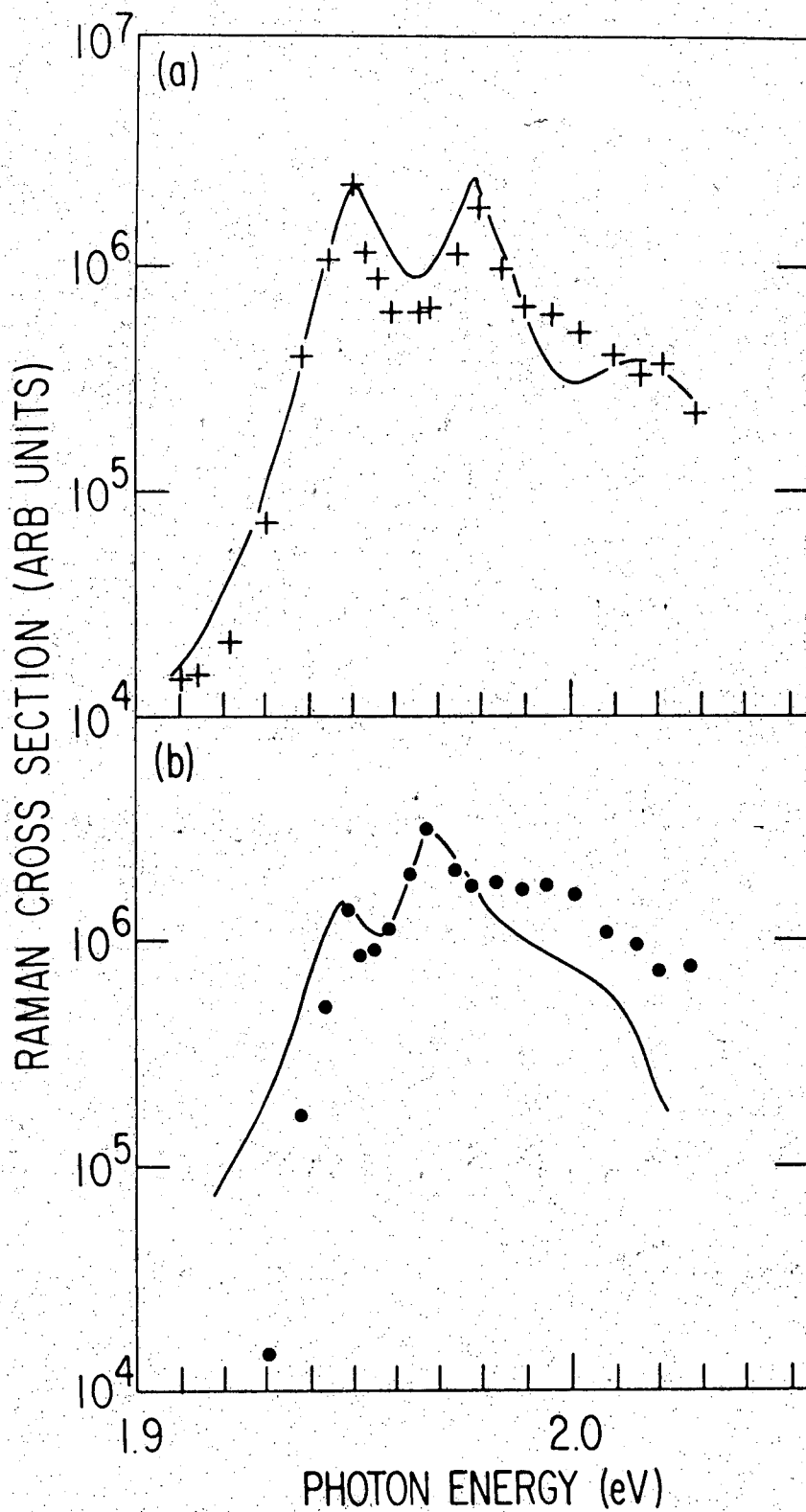


Fig 8

LEGAL NOTICE

This report was prepared as an account of work sponsored by the United States Government. Neither the United States nor the United States Energy Research and Development Administration, nor any of their employees, nor any of their contractors, subcontractors, or their employees, makes any warranty, express or implied, or assumes any legal liability or responsibility for the accuracy, completeness or usefulness of any information, apparatus, product or process disclosed, or represents that its use would not infringe privately owned rights.

TECHNICAL INFORMATION DIVISION
LAWRENCE BERKELEY LABORATORY
UNIVERSITY OF CALIFORNIA
BERKELEY, CALIFORNIA 94720